THE OPEN BOOK SERIES 5

Gauge Theory and Low-Dimensional Topology: Progress and Interaction

Khovanov homology and strong inversions

Artem Kotelskiy, Liam Watson and Claudius Zibrowius

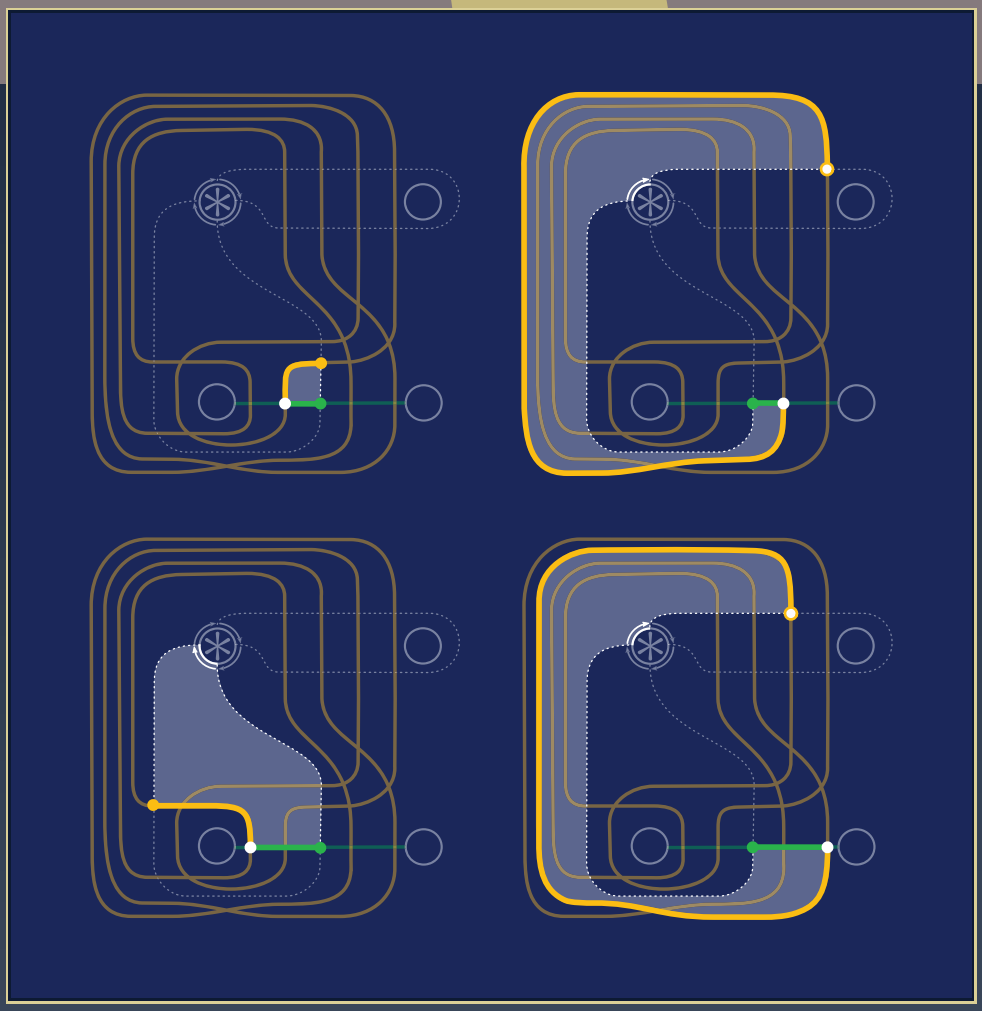

msp

THE OPEN BOOK SERIES **5** (2022)
Gauge theory and low-dimensional topology: progress and interaction
https://doi.org/10.2140/obs.2022.5.223

msp

Khovanov homology and strong inversions

Artem Kotelskiy, Liam Watson and Claudius Zibrowius

There is a one-to-one correspondence between strong inversions on knots in the three-sphere and a special class of four-ended tangles. We compute the reduced Khovanov homology of such tangles for all strong inversions on knots with up to 9 crossings, and discuss these computations in the context of earlier work by the second author (*Adv. Math.* **313** (2017), 915–946). In particular, we provide a counterexample to Conjecture 29 therein, as well as a refinement of and additional evidence for Conjecture 28.

The Brieskorn spheres $\Sigma(2, q, 2nq \mp 1)$ may be obtained by Dehn surgery on a torus knot in the three-sphere, namely, these are the integer homology spheres $S^3_{\pm 1/n}(T_{2,q})$, where $T_{2,q}$ is the positive $(2, q)$ torus knot. These homology spheres admit Seifert fibrations, with base orbifold $S^2(2, q, 2nq \mp 1)$. Denoting by $\mathbf{\Sigma}(A, b)$ the two-fold branched cover of A with branch set b, each of these manifolds admits two descriptions as a two-fold branched cover:

$$S^3_{\pm 1/n}(T_{2,q}) \cong \mathbf{\Sigma}(S^3, T^*_{q,2qn\mp 1}) \cong \mathbf{\Sigma}(S^3, \tau(\pm 1/n)).$$

This construction might be best termed as classical; for our purposes it is helpful to review the notation introduced in [9]. The first of these two-fold branched covers results from an involution on the Seifert fibred space that preserves an orientation on the fibres — we refer to this as the Seifert involution. The second of these arises from the Montesinos involution, which reverses an orientation on the fibres; the branch set in question arises from the Montesinos trick, that is, by first constructing a tangle (B^3, τ) over which the exterior of $T_{2,q}$ is realized as a two-fold branched cover. We review the construction below as it is central to our enumeration of

Kotelskiy is supported by an AMS-Simons travel grant. Watson is supported by an NSERC discovery/accelerator grant. Zibrowius is supported by the Emmy Noether Programme of the DFG, Project number 412851057.
MSC2020: 57K10, 57K18.
Keywords: Khovanov homology, strong inversion, tangle, immersed curves.

tangles. In particular, the branch set $\tau(\pm 1/n)$ is an explicit Montesinos link, which despite the notation depends on q. Generically, these two branch sets are distinct knots. For example, when $q = 5$ and $n = 1$ we have

$$S^3_{+1}(T_{2,5}) \cong \mathbf{\Sigma}(S^3, T^*_{5,9}) \cong \mathbf{\Sigma}(S^3, \tau(+1))$$

and it can be calculated that

$$\dim \widetilde{\mathrm{Kh}}(T^*_{5,9}) = 57 > 15 = \dim \widetilde{\mathrm{Kh}}(\tau(+1)),$$

where the reduced Khovanov homology is taken over the two-element field $\mathbb{F}$. (The Montesinos branch set when $q = 5$ is shown on the right, and the construction of the tangle in this case is reviewed in Figure 1.) This example serves to answer a question due to Ozsváth in the negative: The total dimension of the mod 2 reduced Khovanov homology is not an invariant of two-fold branched covers [9].

This paper focusses on tangles admitting knot exteriors as two-fold branched covers, and the immersed curves that arise as the reduced Khovanov invariants of these tangles [5]. Coefficients are restricted to $\mathbb{F}$ throughout.

1. Strong inversions

A knot K in S^3 is invertible if it admits an isotopy exchanging a choice of orientation on K with the reverse of this choice. A strong inversion is an inversion realized by an involution of the three-sphere. Note that invertible knots which are not strongly invertible exist [4], but that when restricting to hyperbolic knots the two symmetries are equivalent. Following Sakuma [8], given a knot K and a strong inversion h, we will call the pair (K, h) a strongly invertible knot. Strongly invertible knots (K, h) and (K', h') are equivalent if there exists an orientation preserving homeomorphism f on S^3 for which $f(K) = K'$ (so that K and K' are equivalent knots) and $h = f^{-1} \circ h' \circ f$. Alternatively, a strong inversion on a given knot may be viewed as the conjugacy class of an order-two element of the mapping class group of the exterior of the knot; this mapping class group is known as the symmetry group of the knot K. For hyperbolic knots, this group is a subgroup of a dihedral group; see [8, Proposition 3.1].

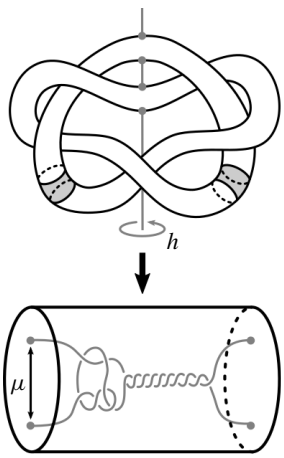

Figure 1. The cinqfoil exterior as a 2-fold branched cover.

A strong inversion gives rise to an involution on a knot's exterior with one-dimensional fixed point set meeting the boundary in exactly 4 points. Note that, according to the Smith conjecture, given an involution on the three-sphere with one-dimensional fixed point set, the fixed point set is unknotted; as a result the fixed point set of the strong inversion on the exterior is a pair of unknotted arcs. Taking the quotient of the order two action on the knot exterior gives rise to a three ball $B^3 = (S^3 \setminus \nu(K))/h$, and the image of the fixed point set of the strong inversion gives rise to a pair of properly embedded arcs $\tau = \mathrm{Im}(\mathrm{Fix}(h))$. Therefore, given a strongly invertible knot, the knot exterior may be viewed as a two-fold branched cover over a four-ended tangle τ in a three ball: $h \curvearrowright (S^3, K)$ so that $S^3 \setminus \nu(K) \cong \mathbf{\Sigma}(B^3, \tau)$. We refer to the tangle $T = (B^3, \tau)$ as the associated quotient tangle to a given knot with strong inversion; see Figure 1 for an explicit example.

In this context, the natural notion of equivalence on tangles is homeomorphism of the pair (B^3, τ) where the boundary is fixed only set-wise. Note that this is, of course, more flexible than the requirement that the boundary be fixed point-wise as is perhaps more common when considering tangle diagrams. In order to be clear about the distinction, we will refer to this latter as a framed tangle. We remark that [9, Definition 3] gives a third notion of equivalence by introducing sutured tangles. This object will not play an explicit role here, however, consulting Figure 1 the reader may find that sutures are a helpful tool for tracking the image of the knot meridian μ in the quotient.

From this point of view, there is a distinguished *trivial* tangle obtained as the quotient of a solid torus, that is, the associated quotient tangle for the trivial knot. The equivalence class of this tangle is the rational tangle. We will have need for choices of representatives $Q_{p/q}$ as described in Figure 2: For any $p/q \in \mathbb{Q}\mathrm{P}^1$, there is a framed tangle diagram $Q_{p/q}$. This choice will allow us to make use of the Montesinos trick:

$$S^3_{p/q}(K) \cong \mathbf{\Sigma}(S^3, \tau(p/q)),$$

where p/q-surgery along the knot K corresponds to the knot $\tau(p/q)$ obtained by gluing the $-p/q$-rational tangle $Q_{-p/q}$ to the tangle τ as in Figure 2 (bottom).

In particular, we are fixing a preferred representative for our associated quotient tangle once and for all: Given (K, h), this is the tangle $T = (B^3, \tau)$ such that the rational closure $\tau(0)$ corresponds to surgery along the Seifert longitude and $\tau(\infty)$ corresponds to $S^3_\infty(K) \cong S^3$. The former implies that the determinant of $\tau(0)$ vanishes, while the latter implies that $\tau(\infty)$ is the unknot, as observed above. (These are also the conditions we check in practice to determine the correct framing.) In fact, there is a bijection between equivalence classes of nontrivial strongly invertible knots (K, h) and tangles (B^3, τ) for which $\tau(\infty)$ is unknotted (this follows from [3, Theorem 2]; compare [10, Proposition 9]). As such, associated quotient tangles provide an invariant of strong inversions.

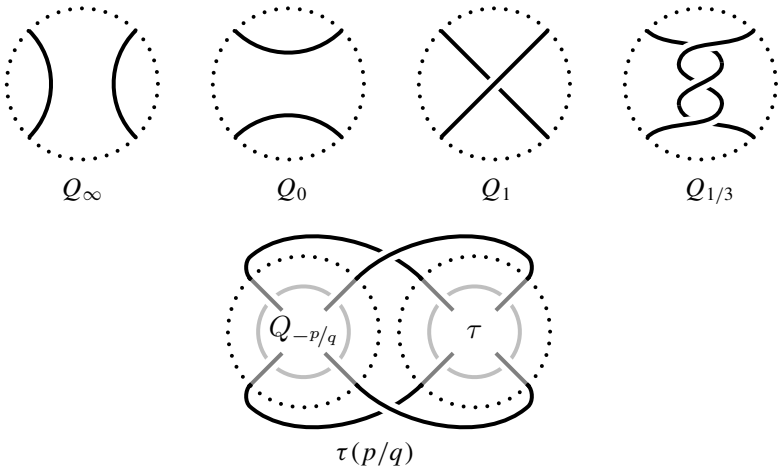

Figure 2. Examples of framed rational tangles (top) and the rational closure of a four-ended tangle τ (bottom).

Strong inversions give a means of enumerating interesting tangles, and we use this strategy below. Observe that, given a hyperbolic knot admitting a pair of distinct strong inversions h_1 and h_2, by Thurston's hyperbolic Dehn filling theorem, $S^3_{p/q}(K)$ is hyperbolic for all but finitely many slopes p/q. Moreover

$$\mathbf{\Sigma}(S^3, \tau_1(p/q)) \cong S^3_{p/q}(K) \cong \mathbf{\Sigma}(S^3, \tau_2(p/q))$$

and, generically, the branch sets $\tau_1(p/q)$ and $\tau_2(p/q)$ are distinct knots. It is a striking fact that for all K with fewer than 9 crossings

$$\dim \widetilde{\mathrm{Kh}}(\tau_1(p/q)) = \dim \widetilde{\mathrm{Kh}}(\tau_2(p/q)),$$

that is, finding a negative answer to Ozsváth's question in the hyperbolic setting is surprisingly difficult. This observation follows from Theorem 3.2 below.

A range of examples of strong inversions and associated quotient tangles are considered in [10]. We will expand this list in a systematic way below, and highlight in particular the knot 9_{46} in the Rolfsen table; see Figure 3. It is worth noting that these tangles distinguish the strong inversions in question: Ignoring one strand, the second tangle contains 8_{19} as a subknot, while the only subknots in the first tangle are trefoils.

In the context of the discussion above, it seems natural to try and articulate a relative version of Ozsváth's question. In particular, are there Khovanov-type tangle invariants that are invariants of the knot K independent on the chosen strong inversion h? We will see that 9_{46} dashes any hope of this (see Counterexample 3.8) and, furthermore, provides hyperbolic counterexamples to Ozsváth's original question (see Remark 3.3).

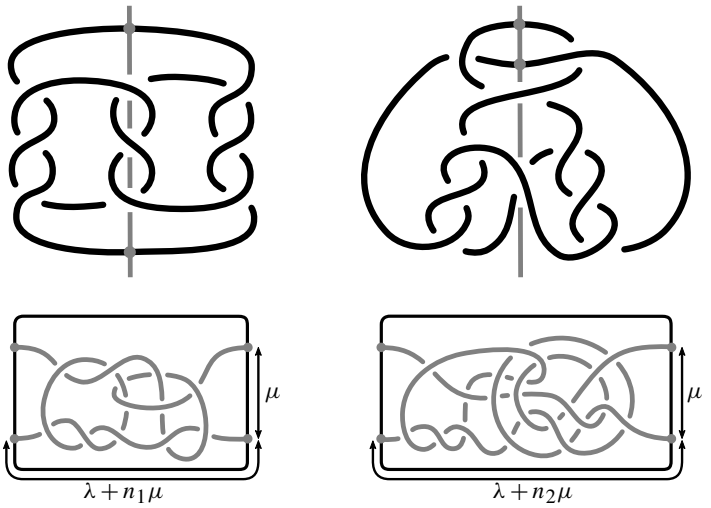

Figure 3. Two strong inversions on the knot 9_{46} (top row) together with the associate quotient tangle for each (bottom row). In order to present minimal crossing diagrams for the associated quotient tangles, this is the one place where we present something other than the preferred tangle representative: The first symmetry gives rise to a tangle T_1 shown with framing $n_1 = 2$, while the second symmetry gives rise to a tangle T_2 with framing $n_2 = -6$.

Interestingly, 9_{46} also makes a star appearance in the recent work of Boyle and Issa [2]. In particular, this knot is slice, but it has nonzero equivariant four-genus; see [2, Figure 14] and the surrounding discussion.

2. Review of the tangle invariants $\widetilde{\mathrm{Kh}}$ and $\widetilde{\mathrm{BN}}$

Let T be a four-ended tangle in the three-ball B^3. In earlier work we interpreted the Bar–Natan tangle invariant $[\![T]\!]_{/l}$ in terms of *multicurves*, that is, isotopy classes of collections of immersed curves in the four-punctured sphere $\partial B^3 \smallsetminus \partial T$ [1; 5]. After choosing a distinguished tangle end $*$ of T, the construction outputs two multicurve-valued invariants $\widetilde{\mathrm{Kh}}(T)$ and $\widetilde{\mathrm{BN}}(T)$:

$$T \overset{[1]}{\longmapsto} [\![T]\!]_{/l} \overset{[5]}{\longmapsto} \widetilde{\mathrm{Kh}}(T),\ \widetilde{\mathrm{BN}}(T) \looparrowright S^2_{4,*} = \partial B^3 \smallsetminus \partial T.$$

These multicurves are equipped with a bigrading, which we expand on below. Also, strictly speaking, components of $\widetilde{\mathrm{BN}}(T)$ come equipped with local systems. However, in this paper, we will suppress this subtlety, since over $\mathbb{F}$ these local systems are trivial in all known examples.

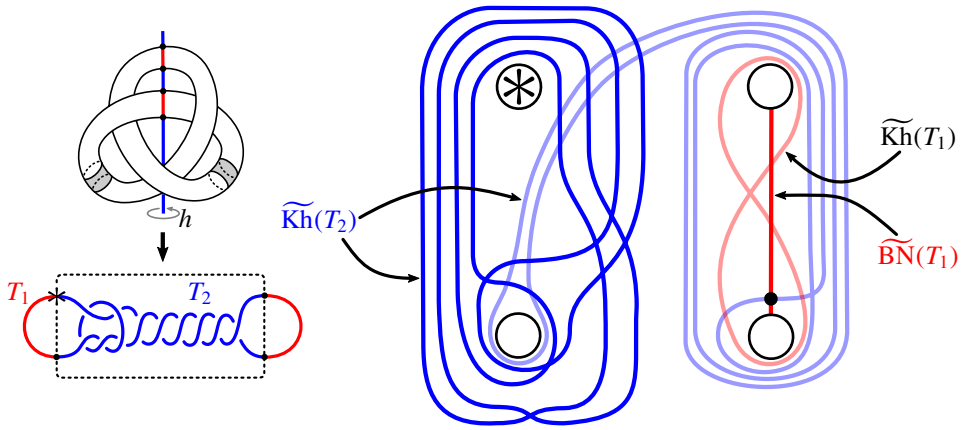

Figure 4. Illustrated on the left is the trefoil with strong inversion, highlighting the decomposition of the unknot into tangles T_1 and T_2, where T_2 is the preferred representative of the associated quotient tangle to the strong inversion. The corresponding intersection picture is shown on the right, where all of the relevant information has been projected to the front face of the sphere: The Lagrangian Floer homology $\mathrm{HF}(\widetilde{\mathrm{BN}}(T_1), \widetilde{\mathrm{Kh}}(T_2)) = \mathbb{F}$ recovers the one-dimensional reduced Khovanov homology of the unknot.

The curve invariants enjoy the following gluing property [5, Theorem 1.9]: Given a decomposition of a knot $K = T_1 \cup T_2$ into four-ended tangles, the reduced Khovanov homology of the knot is recovered via Lagrangian Floer homology:

$$\widetilde{\mathrm{Kh}}(K) \cong \mathrm{HF}(\mathrm{m}(\widetilde{\mathrm{BN}}(T_1)), \widetilde{\mathrm{Kh}}(T_2)) \tag{1}$$

where m is the map identifying the two four-punctured spheres. An example illustrating this gluing formula is given in Figure 4.

Let us recall some basic facts about $\widetilde{\mathrm{Kh}}(T)$ and $\widetilde{\mathrm{BN}}(T)$ from [5, Section 6]: Both invariants may consist of multiple components. A component is either an immersion of a circle or an immersion of an interval. In the first case we call a component compact; in the second, noncompact. The invariant $\widetilde{\mathrm{BN}}(T)$ contains exactly one noncompact component (unless the tangle T contains some closed component, which is not the case in the present context), whereas $\widetilde{\mathrm{Kh}}(T)$ consists only of compact components. These curves become easier to manage when considered in a certain covering space of $S^2_{4,*}$, namely the planar cover that factors through the toroidal two-fold cover:

$$(\mathbb{R}^2 \smallsetminus \mathbb{Z}^2) \to (T^2 \smallsetminus 4\mathrm{pt}) \to S^2_{4,*}$$

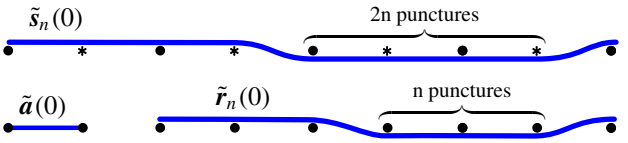

Figure 5. The curves $\tilde{\boldsymbol{a}}(0)$, $\{\tilde{\boldsymbol{s}}_n(0)\}_{n\geqslant 1}$, and $\{\tilde{\boldsymbol{r}}_n(0)\}_{n\geqslant 1}$.

Definition 2.1. Given an immersed curve $c \looparrowright S^2_{4,*}$, denote by $\tilde{c}$ a lift of c to the cover $\mathbb{R}^2 \smallsetminus \mathbb{Z}^2$. For $n \in \mathbb{N}$, let $\boldsymbol{a}(0)$, $\boldsymbol{r}_n(0)$, and $\boldsymbol{s}_{2n}(0)$ be the immersed curves in $S^2_{4,*}$ that respectively admit lifts to the curves $\tilde{\boldsymbol{a}}(0)$, $\tilde{\boldsymbol{r}}_n(0)$, and $\tilde{\boldsymbol{s}}_{2n}(0)$ in Figure 5. For every $p/q \in \mathbb{Q}\mathrm{P}^1$, we respectively define the curves $\boldsymbol{a}(p/q)$, $\boldsymbol{r}_n(p/q)$, and $\boldsymbol{s}_{2n}(p/q)$ as the images of $\boldsymbol{a}(0)$, $\boldsymbol{r}_n(0)$, and $\boldsymbol{s}_{2n}(0)$ under the action of

$$\begin{bmatrix} q & r \\ p & s \end{bmatrix}$$

considered as an element of the mapping class group fixing the special puncture $\mathrm{Mod}(S^2_{4,*}) \cong PSL(2,\mathbb{Z})$, where $qs - pr = 1$. (This transformation maps straight lines of slope 0 to straight lines of slope p/q.) We call $\boldsymbol{a}(p/q)$ a *rational arc of slope* p/q; we call $\boldsymbol{r}_n(p/q)$ a curve of *rational type*, *slope* p/q, *and length* n; and $\boldsymbol{s}_{2n}(p/q)$ a curve of *special type*, *slope* p/q, *and length* $2n$.

Example 2.2. The curve $\widetilde{\mathrm{Kh}}(T_2)$ from Figure 4 consists of the special component $\boldsymbol{s}_4(\infty)$ and the rational component $\boldsymbol{r}_1(4)$. Furthermore, $\widetilde{\mathrm{BN}}(T_1) = \{\boldsymbol{a}(\infty)\}$ is the red vertical arc, while $\widetilde{\mathrm{Kh}}(T_1) = \{\boldsymbol{r}_1(\infty)\}$ consists of the figure-eight curve lying in a small neighbourhood of this arc. More generally, justifying the terminology, naturality of the invariants under the mapping class group action [5, Theorem 1.13] implies that $\widetilde{\mathrm{BN}}(Q_{p/q}) = \{\boldsymbol{a}(p/q)\}$ and $\widetilde{\mathrm{Kh}}(Q_{p/q}) = \{\boldsymbol{r}_1(p/q)\}$ — so, rational tangles have rational invariants.

The invariants $\widetilde{\mathrm{BN}}(T)$ and $\widetilde{\mathrm{Kh}}(T)$ are topological interpretations of algebraic invariants $\mathit{Д}(T)$ and $\mathit{Д}_1(T)$, respectively, which are type D structures over the algebra $\mathcal{B}$. For example, the curve $\boldsymbol{s}_4(\infty)$, which is the blue curve on the left of Figure 7, corresponds to the type D structure in Figure 6; the arc $\boldsymbol{a}(0)$ corresponds to the one-generator complex $[{}^0\bullet_0]$. To translate between these two viewpoints, we need to fix a parametrization of the four-punctured sphere $S^2_{4,*}$, which is indicated by the two grey dashed arcs in Figure 7. Briefly, intersection points of these arcs with a given curve give rise to the generators of the corresponding type D structure and paths between intersection points determine the differential; for more details, see [5, Example 1.6]. The generators of the type D structures carry a bigrading, that is a quantum grading q and a homological grading h. We indicate these gradings on generators $\bullet$ and the corresponding intersection points by super- and subscripts like so: ${}^q\bullet_h$. Also the algebra $\mathcal{B}$ is equipped with quantum and homological

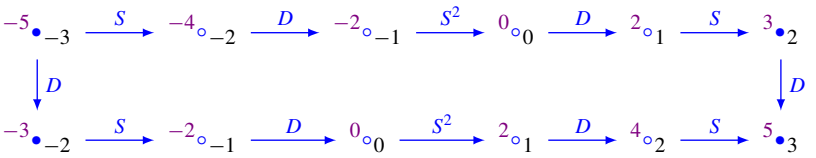

Figure 6. The symmetrically bigraded type D structure corresponding to the special curve $s_{4n}(\infty)$ for $n = 1$. The type D structures for $n > 1$ look similar. The total number of generators in idempotent $\circ$ is equal to $8n$. The absolute bigrading is fixed by requiring that the minimal and maximal homological and quantum gradings are $\pm(2n+1)$ and $\pm(4n+1)$, respectively.

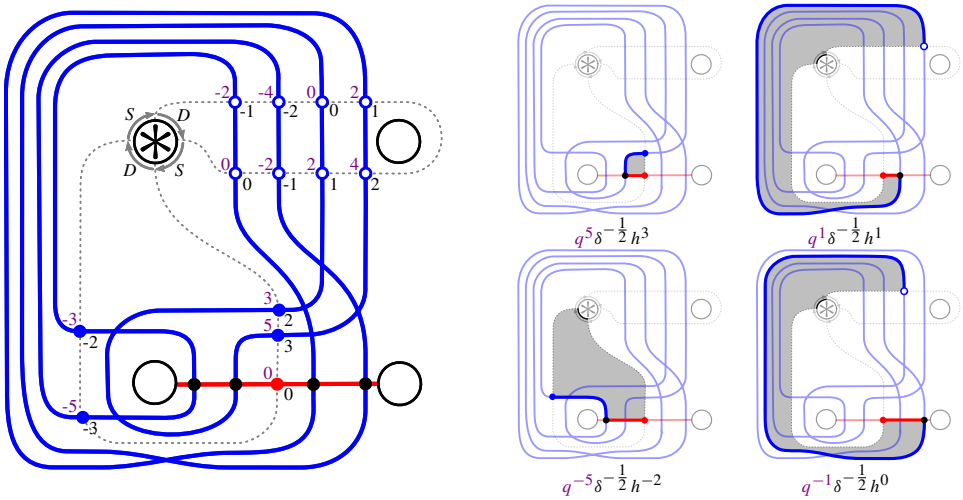

Figure 7. Computing the gradings associated with the four-dimensional vector space $\mathrm{HF}(\boldsymbol{a}(0), s_4(\infty))$, according to Lemma 2.5.

gradings, which are determined by $q(D) = 2q(S) = -2$, $h(D) = h(S) = 0$. The differentials of type D structures reduce homological grading by 1 and preserve the quantum grading, namely if there is an arrow $x \xrightarrow{a} y$ in the differential, then $q(y)+q(a)-q(x) = 0$, $h(y)+h(a)-h(x) = 1$. Thus, the bigrading of any given component of a multicurve is determined by the bigrading of a single generator which lies on this component.

The bigradings on $\widetilde{\mathrm{BN}}(T)$ and $\widetilde{\mathrm{Kh}}(T)$ depend on an orientation of the tangle T. This dependence is discussed in [5, Proposition 4.8]. If T is an unoriented tangle, $\widetilde{\mathrm{BN}}(T)$ and $\widetilde{\mathrm{Kh}}(T)$ only carry *relative* bigradings, i.e., bigradings that are well-defined up to an overall shift. For tangles whose components have linking number 0, such as the trivial tangle  , all orientations induce the same bigrading.

Theorem 2.3 [6, Theorem 2.15]. *For any pointed Conway tangle T, every component of $\widetilde{\mathrm{Kh}}(T)$ is equal to $\boldsymbol{r}_n(p/q)$ or $\boldsymbol{s}_{2n}(p/q)$ for some $n \in \mathbb{N}$ and $p/q \in \mathbb{Q}\mathrm{P}^1$, up to some bigrading shift. In other words, components of $\widetilde{\mathrm{Kh}}(T)$ are completely classified by their type, slope, length, and bigrading.*

In the context of Heegaard Floer homology, analogous properties are known for the tangle invariant $\mathrm{HFT}(T)$ [11]. Note, however, that components of the invariant $\widetilde{\mathrm{BN}}(T)$ are known to be much more complicated even when restricting to only compact components.

We conclude this section with a computation of the Lagrangian Floer intersection pairing between a simple arc and the special curves $\boldsymbol{s}_{4n}(\infty)$, which will play a central role later.

Definition 2.4. Define $V_\varkappa$ as the four-dimensional bigraded vector space supported in δ-grading 0 and quantum gradings -5, -1, $+1$, and $+5$.

Lemma 2.5. *We have*

$$\mathrm{HF}(\boldsymbol{a}(0), \boldsymbol{s}_4(\infty)) \cong q^0\delta^{-\frac{1}{2}}h^{\frac{1}{2}}V_\varkappa.$$

More generally, for any positive integer n,

$$\mathrm{HF}(\boldsymbol{a}(0), \boldsymbol{s}_{4n}(\infty)) \cong \bigoplus_{i=1}^{n} q^{4(2i-n-1)}\delta^{-\frac{1}{2}}h^{\frac{1}{2}+2(2i-n-1)}V_\varkappa.$$

In both cases, the isomorphism holds as absolutely bigraded vector spaces if $\boldsymbol{s}_{4n}(\infty)$ is symmetrically bigraded (in the sense of Figure 6) *and $\boldsymbol{a}(0)$ agrees with $\widetilde{\mathrm{BN}}$*() *as a **bigraded** curve.*

Proof. The total dimension of $\mathrm{HF}(\boldsymbol{a}(0), \boldsymbol{s}_{4n}(\infty))$ is $4n$, since the minimal number of intersection points between the two curves is $4n$. For the computation of the bigrading, we will focus on the case $n = 1$; the case $n > 1$ is similar. Recall how this works [5, Section 7.2]: The bigrading of an intersection point $\bullet$ generating $\mathrm{HF}(\boldsymbol{a}(0), \boldsymbol{s}_4(\infty))$ is computed by considering a path on $\boldsymbol{a}(0) \cup \boldsymbol{s}_4(\infty)$ which starts at $x = {}^{0}\bullet_{0}$, turns right at the intersection point $\bullet$ and ends at the nearest intersection point $y = {}^{q}\circ_{h}$ or $y = {}^{q}\bullet_{h}$ of $\boldsymbol{s}_4(\infty)$ with the parametrization. These paths are illustrated on the right of Figure 7. Each of these paths in $S^2_{4,*}$ is homotopic relative to the parametrizing arcs to some path γ on the boundary of the special puncture; these homotopies are indicated on the right of Figure 7 by the shaded disks. We set $q(\gamma) = 0, -1, -2$, depending on whether the path γ is constant, equal to S, or equal to D, respectively. (More generally, these paths correspond to some algebra elements in $\mathcal{B}$, whose quantum gradings define $q(\gamma)$.) Then

$$h(\bullet) = h(y) - h(x) \quad \text{and} \quad q(\bullet) = q(y) - q(x) + q(\gamma).$$

Finally, we compute the δ-grading from the identity $\delta + h = \frac{1}{2}q$. □

3. The Khovanov homology of strong inversions

A strongly invertible knot (K, h) gives rise to an associated four-ended quotient tangle $T = (B^3, \tau)$. (When we have need for it, we will use the notation $T_{K,h}$ to remember the dependence on the strongly invertible knot.) We use the same preferred framing as in Section 1; in particular, $\tau(\infty)$ is the unknot. This imposes strong restrictions on the curve invariant $\widetilde{\mathrm{Kh}}(T)$, namely, it implies that

$$\widetilde{\mathrm{Kh}}(\tau(\infty)) = \mathrm{HF}\big(\widetilde{\mathrm{BN}}(\quad), \widetilde{\mathrm{Kh}}(T)\big) = \mathrm{HF}(\boldsymbol{a}(\infty), \widetilde{\mathrm{Kh}}(T)) = \mathbb{F}.$$

In other words, $\widetilde{\mathrm{Kh}}(T)$ is homotopic to a multicurve that intersects the arc $\boldsymbol{a}(\infty)$ only once, as is the case for the example $\widetilde{\mathrm{Kh}}(T_2)$ from Figure 4. In the light of the classification given in Theorem 2.3, this implies:

Theorem 3.1. *Let h be a strong inversion on a knot $K \subset S^3$. Then*

$$\widetilde{\mathrm{Kh}}(T_{K,h}) = \boldsymbol{r}_1(k) \cup \boldsymbol{s}_{2n_1}(\infty) \cup \cdots \cup \boldsymbol{s}_{2n_N}(\infty)$$

for some integers $k \in \mathbb{Z}$ and $N, n_1, \ldots, n_N \in \mathbb{Z}_{>0}$. □

In fact, with the help of a computer [12], we show the following:

Theorem 3.2. *Let h be a strong inversion on a knot $K \subset S^3$ with at most 9 crossings. With notation as in Theorem 3.1, k is divisible by 4 and $n_i = 2$ for $i = 1, \ldots, N$.* □

Table 1 shows the ungraded invariants for all pairs (K, h) from Theorem 3.2; the bigraded invariants are listed in Section 4. To determine the absolute bigrading, we use the braid-like orientation on $T_{K,h}$. Note that, in order to match Sakuma's table [8], the first row in Table 1 describes the left-hand trefoil and its rational component has slope -4, while Figure 4 depicts the right-hand trefoil and its rational component has slope 4. Among tabulated knots through 9 crossings, there are 57 knots that admit two distinct strong inversions. For all but one of these knots with two distinct strong inversions, the ungraded invariants $\widetilde{\mathrm{Kh}}(T)$ agree; these pairs of strong inversions are indicated in Table 1 by the superscript $\spadesuit$.

Remark 3.3. The knot 9_{46} is the only knot in this collection whose strong inversions 9^1_{46} and 9^2_{46} can be distinguished by their ungraded invariants $\widetilde{\mathrm{Kh}}(T)$, as shown in the two highlighted rows in Table 1. Here, we follow the same numbering convention for strong inversions as in [8]. Note that both the slope k and the number n of special components $\boldsymbol{s}_4(\infty)$ distinguish 9^1_{46} and 9^2_{46}. With this example in hand, one can check that $\dim \widetilde{\mathrm{Kh}}(\tau_1(n)) \neq \dim \widetilde{\mathrm{Kh}}(\tau_2(n))$ by applying the pairing formula (1), despite the fact that $\boldsymbol{\Sigma}(S^3, \tau_1(n)) \cong \boldsymbol{\Sigma}(S^3, \tau_2(n))$ by construction. Calculations for $\dim \widetilde{\mathrm{Kh}}(\tau_i(p/q))$ with $i = 1, 2$ can be obtained as well with a little more patience.

3_1	−4	1	$8_4^\spadesuit$	−4	9	9_1	−16	4	$9_{18}^\spadesuit$	−8	20	$9_{37}^\spadesuit$	0	22
$4_1^\spadesuit$	0	2	$8_5^\spadesuit$	8	10	$9_2^\spadesuit$	−4	7	$9_{19}^\spadesuit$	0	20	9_{38}	−8	28
5_1	−8	2	$8_6^\spadesuit$	−4	11	$9_3^\spadesuit$	12	9	$9_{20}^\spadesuit$	−8	20	9_{39}	4	27
$5_2^\spadesuit$	−4	3	$8_7^\spadesuit$	4	11	$9_4^\spadesuit$	−8	10	$9_{21}^\spadesuit$	4	21	$9_{40}^\spadesuit$	−4	37
$6_1^\spadesuit$	0	4	$8_8^\spadesuit$	0	12	$9_5^\spadesuit$	4	11	9_{22}	4	21	9_{41}	0	24
$6_2^\spadesuit$	−4	5	$8_9^\spadesuit$	0	12	$9_6^\spadesuit$	−12	13	$9_{23}^\spadesuit$	−8	22	9_{42}	0	4
$6_3^\spadesuit$	0	6	8_{10}	4	13	$9_7^\spadesuit$	−8	14	9_{24}	0	22	9_{43}	8	6
7_1	−12	3	$8_{11}^\spadesuit$	−4	13	$9_8^\spadesuit$	−4	15	9_{25}	−4	23	9_{44}	0	8
$7_2^\spadesuit$	−4	5	$8_{12}^\spadesuit$	0	14	$9_9^\spadesuit$	−12	15	$9_{26}^\spadesuit$	4	23	9_{45}	−4	11
$7_3^\spadesuit$	8	6	$8_{13}^\spadesuit$	0	14	$9_{10}^\spadesuit$	8	16	$9_{27}^\spadesuit$	0	24	9_{46}^1	0	4
$7_4^\spadesuit$	4	7	$8_{14}^\spadesuit$	4	15	$9_{11}^\spadesuit$	8	16	$9_{28}^\spadesuit$	−4	25	9_{46}^2	−4	7
$7_5^\spadesuit$	−8	8	$8_{15}^\spadesuit$	−8	16	$9_{12}^\spadesuit$	−4	17	9_{29}	−4	25	9_{47}	4	13
$7_6^\spadesuit$	−4	9	8_{16}	−4	17	$9_{13}^\spadesuit$	8	18	9_{30}	0	26	$9_{48}^\spadesuit$	−4	13
$7_7^\spadesuit$	0	10	$8_{18}^\spadesuit$	0	22	$9_{14}^\spadesuit$	0	18	$9_{31}^\spadesuit$	4	27	9_{49}	8	12
$8_1^\spadesuit$	0	6	8_{19}	8	2	$9_{15}^\spadesuit$	4	19	9_{34}	0	34			
$8_2^\spadesuit$	−8	8	8_{20}	0	4	$9_{16}^\spadesuit$	12	19	$9_{35}^\spadesuit$	−4	13			
$8_3^\spadesuit$	0	8	$8_{21}^\spadesuit$	−4	7	$9_{17}^\spadesuit$	−4	19	9_{36}	8	18			

Table 1. The ungraded reduced Khovanov homology of the tangles $T_{K,h}$ associated with strong inversions h on all prime knots K with up to 9 crossings. There are three columns in this table. The first specifies the knots K. Those marked by a superscript $\spadesuit$ admit two distinct strong inversions, and the associated ungraded invariants agree (and are hence listed together). The knot 9_{46} admits two strong inversions, but their invariants are distinct; see the two highlighted rows. All remaining knots admit only a single strong inversion. The second column specifies the slope k of the single rational component $\boldsymbol{r}_1(k)$ in $\widetilde{\mathrm{Kh}}(T_{K,h})$, and the third column gives the number N of special components, all of which are equal to $\boldsymbol{s}_4(\infty)$.

As stated in Section 2, $\widetilde{\mathrm{Kh}}(T)$ for a general four-ended tangle only consists of rational and special curves; it would be interesting to give a geometric interpretation for the slopes of these curves. For quotient tangles $T_{K,h}$ of strong inversions (K, h), the existence of the unknot closure implies that the slope of any special curve is fixed and the slope of the rational component is an integer. As we can see from the second column in Table 1, this integer may be nonzero; in other words, the slope of the rational component of $\mathrm{Kh}(T_{K,h})$ need not agree with the slope given by the rational longitude of the knot K. Our computations raise the following:

Questions 3.4. *Is there a geometric/topological meaning of the slope of the rational component of* $\widetilde{\mathrm{Kh}}(T_{K,h})$? *Is the slope always divisible by* 4?

We now focus on the special components:

Definition 3.5. Given a knot with a strong inversion (K, h), let $\boldsymbol{s}(K, h)$ be the set of special components of $\widetilde{\mathrm{Kh}}(T_{K,h})$. Let $\boldsymbol{a}(0) = \widetilde{\mathrm{BN}}\left(\text{⊗}\right)$ as in Figure 7. Then define

$$\varkappa(K, h) := \mathrm{HF}(\boldsymbol{a}(0), \boldsymbol{s}(K, h))$$

In [10], the second author defined an invariant of the same name. The following lemma justifies our notation:

Lemma 3.6. *The invariant* $\varkappa(K, h)$ *agrees with the invariant from* [10] *as a relatively bigraded vector space.*

Proof. The original invariant $\varkappa(K, h)$ was defined as a certain finite-dimensional quotient of the inverse limit $\varprojlim \widetilde{\mathrm{Kh}}(\tau(n))$ associated with the maps

$$\widetilde{\mathrm{Kh}}(\tau(n+1)) \to \widetilde{\mathrm{Kh}}(\tau(n))$$

induced by resolving a crossing [10, Proposition 11]. Since this inverse limit is determined by the maps for positive n we can assume in the following that $n > 0$. By the gluing property of the multicurve tangle invariants,

$$\widetilde{\mathrm{Kh}}(\tau(n)) \cong \mathrm{HF}(\boldsymbol{a}(n), \widetilde{\mathrm{Kh}}(\tau))$$

The right-hand side can also be interpreted as the homology of the morphism space between the type D structures associated with $\boldsymbol{a}(n)$ and $\widetilde{\mathrm{Kh}}(\tau)$ [5, Theorem 1.5]. Gluing is functorial; in fact, the map

$$\mathrm{HF}(\boldsymbol{a}(n+1), \widetilde{\mathrm{Kh}}(\tau)) \xrightarrow{\cong} \widetilde{\mathrm{Kh}}(\tau(n+1)) \to \widetilde{\mathrm{Kh}}(\tau(n)) \xrightarrow{\cong} \mathrm{HF}(\boldsymbol{a}(n), \widetilde{\mathrm{Kh}}(\tau))$$

is induced by precomposition with the following morphism from the type D structure for $\boldsymbol{a}(n)$ to the type D structure for $\boldsymbol{a}(n+1)$:

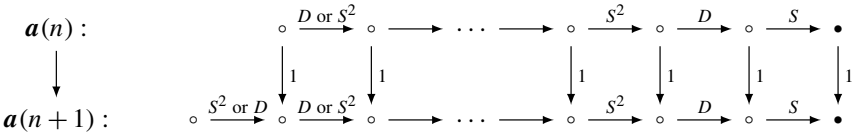

(2)

This can be seen explicitly by induction or by observing that the Lagrangian Floer homology $\mathrm{HF}(\boldsymbol{a}(n), \boldsymbol{a}(n+1))$ computes the Bar–Natan homology of the unknot, so there is only one nonzero equivalence class of morphisms in the correct quantum grading.

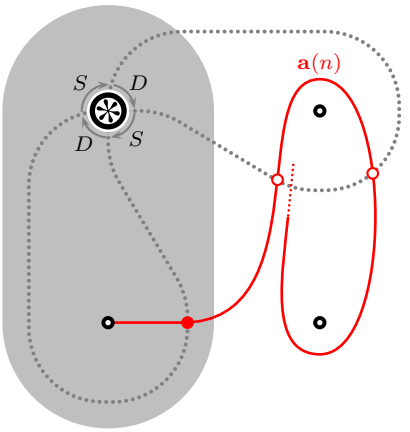

Figure 8. A schematic for the Lagrangian Floer pairing $\mathrm{HF}(\boldsymbol{a}(n), \boldsymbol{s}_{2i}(\infty))$ in the proof of Lemma 3.6: The curve $\boldsymbol{s}_{2i}(\infty)$ can be drawn such that it lies in the shaded region, and so do all the intersection points with $\boldsymbol{a}(n)$. Precomposition with the map (2) induces the identity on the corresponding morphisms.

Now apply the (contravariant) functor $\mathrm{HF}(-, \widetilde{\mathrm{Kh}}(\tau))$ to this map. We can do this for each component of $\widetilde{\mathrm{Kh}}(\tau)$ separately, using Theorem 3.1. First, for any integer k, $\varprojlim \mathrm{HF}(\boldsymbol{a}(n), \boldsymbol{r}_1(k))$ is isomorphic to $\varprojlim \mathrm{HF}(\boldsymbol{a}(n-k), \boldsymbol{r}_1(0))$. The latter computes the invariant of the unknot (with its unique strong inversion), which vanishes by [10, Theorem 1]. Moreover, a simple computation shows that the map

$$\mathrm{HF}(\boldsymbol{a}(n+1), \boldsymbol{s}_{2i}(\infty)) \to \mathrm{HF}(\boldsymbol{a}(n), \boldsymbol{s}_{2i}(\infty))$$

induced by (2) is an isomorphism for any integer $i > 0$; this is illustrated in Figure 8. Thus

$$\varprojlim \mathrm{HF}(\boldsymbol{a}(n), \boldsymbol{s}_{2i}(\infty)) \cong \mathrm{HF}(\boldsymbol{a}(0), \boldsymbol{s}_{2i}(\infty)).$$

Moreover, the subspace that we need to quotient by to obtain the invariant from [10] vanishes. This proves the claim. □

Remark 3.7. Since the maps for the inverse limit $\varprojlim \widetilde{\mathrm{Kh}}(\tau(n))$ preserve the homological grading, the original invariant $\varkappa(K, h)$ carries an absolute (co)homological grading. The identification with our invariant respects this grading, so the two definitions actually give rise to the same absolute homological grading. However, the quantum and δ-gradings on the original invariant are only well-defined as relative gradings. An ad hoc construction to lift these to absolute gradings is discussed in [10, Section 7]. We have not attempted to relate these lifts to the absolute bigrading on our invariant; in general, they do not agree.

Counterexample 3.8. Returning to the pair of strong inversions on the knot 9_{46}, we calculate that

$$\dim \varkappa(K, h_1) = 16 < 28 = \dim \varkappa(K, h_2)$$

contrary to [10, Conjecture 29]. This conjecture was originally posed in the hope that a relative variant of Ozsváth's question might help to explain the examples described in [9], which depend heavily on the Seifert structure. Comparing with Remark 3.3 and the proof of Lemma 3.6, it is worth noting a simple relationship between $\varkappa(K, h)$ and $\widetilde{\mathrm{Kh}}(\tau(n))$ when restricting to the preferred framing: According to Definition 3.5,

$$\dim \widetilde{\mathrm{Kh}}(\tau(n)) = \dim \varkappa(K, h) + \dim \mathrm{HF}(\boldsymbol{a}(n), \boldsymbol{r}_1(k)),$$

where k is as in Theorem 3.2. Note that the second summand is the dimension of the reduced Khovanov homology of the $(2, n-k)$-torus link.

On the other hand, certain structural properties appear to persist:

Conjecture 3.9 [10, Conjecture 28]. *For any strong inversion* (K, h), *the vector space* $\varkappa(K, h)$ *is a direct sum of copies of* $V_\varkappa$. *In particular*, $\dim \varkappa(K, h)$ *is divisible by* 4.

By Lemma 2.5, the vector space $V_\varkappa$ is precisely the Lagrangian Floer homology of the arc $\boldsymbol{a}(0)$ and the special curve $\boldsymbol{s}_4(\infty)$. So a strong inversion (K, h) satisfies Conjecture 3.9 if all special components of $\widetilde{\mathrm{Kh}}(T_{K,h})$ are equal to $\boldsymbol{s}_4(\infty)$ up to a grading shift. In particular, the calculations summarized in Table 1 verify Conjecture 3.9 for all strong inversions on tabulated knots through 9 crossings.

We remark that Conjecture 3.9 implies that the slope of the rational component of $\widetilde{\mathrm{Kh}}(T_{K,h})$ should be divisible by 4 (Questions 3.4, second part). This can be seen as follows. First note that the group $H_1(\boldsymbol{\Sigma}(S^3, \tau(0))) \cong H_1(S^3_0(K))$ has positive rank hence $\det(\tau(0)) = 0$. The determinant of a link can also be computed by evaluating the Jones polynomial at -1, which agrees with the Euler characteristic of Khovanov homology with respect to the δ-grading:

$$\begin{aligned} 0 = \det(\tau(0)) &= |V(-1)| \\ &= |\chi_\delta \widetilde{\mathrm{Kh}}(\tau(0))| = |\chi_\delta \mathrm{HF}(\boldsymbol{a}(0), \widetilde{\mathrm{Kh}}(T))|. \end{aligned}$$

This means that the δ-graded intersections of $\boldsymbol{a}(0)$ with special components cancel out intersections with the rational component. Conjecture 3.9 implies that intersections with special components come in groups of 4 concentrated in a single δ-grading, and so the number of intersections with the rational component — also concentrated in a single δ-grading — should be divisible by 4.

Incorporating Lemma 2.5 gives the following refinement of Conjecture 3.9:

Conjecture 3.10. *The length of any special component of* $\widetilde{\mathrm{Kh}}(T_{K,h})$ *for any strongly invertible knot* (K, h) *is divisible by* 4.

The special components in all examples that we have tabulated are equal to $\boldsymbol{s}_4(\infty)$, but there exist strongly invertible knots (K, h) for which $\widetilde{\mathrm{Kh}}(T_{K,h})$ contains special components $\boldsymbol{s}_{4n}(\infty)$ with $n \neq 1$.

As we can see from Table 1, the ungraded invariant $\varkappa(K, h)$ cannot tell all strong inversions apart. However, the *absolutely bigraded* invariant $\varkappa(K, h)$ can distinguish any pair of strong inversion for knots up to 9 crossings.

Question 3.11 [10, Question 19]. *Is there a hyperbolic knot* $K \subset S^3$ *with two distinct strong inversions that cannot be distinguished by the absolutely bigraded invariant* $\varkappa$?

The restriction to hyperbolic is important here, and was omitted in error in the statement of [10, Question 19]. Note that the question is not interesting for torus knots, as these admit unique strong inversions. However, it is possible to generate satellite knots with strong inversions whose associated quotient tangles differ by mutation on a subtangle. Owing to the insensitivity of Khovanov homology to mutation, such symmetries cannot be separated.

Remark 3.12. Although our focus has been entirely on four-ended tangles admitting an unknot closure, we expect Conjecture 3.10 to hold more generally: For any four-ended tangle T, any special component of $\widetilde{\mathrm{Kh}}(T)$ should be equal to $\boldsymbol{s}_{4n}(p/q)$ for some $p/q \in \mathbb{Q}\mathrm{P}^1$ and $n > 0$.

Remark 3.13. In this paper, we have worked exclusively over the field $\mathbb{F}$ of two elements; all of the above questions should be read with this coefficient system in place. We conclude with a comment about other fields of coefficients. Unlike knot Floer homology, Khovanov homology is known to behave very differently over fields of different characteristic. Many of the conjectures above fail if we work over a field different from $\mathbb{F}$. For example, consider the second strong inversion 7_4^2 on the knot 7_4 in Sakuma's table [8]. Its invariant $\widetilde{\mathrm{Kh}}(T_{7_4^2}; \mathbb{Z}/3)$ consists of a single rational component $\boldsymbol{r}_1(6)$, two special components $\boldsymbol{s}_4(\infty)$, but also five special components $\boldsymbol{s}_2(\infty)$. So the corresponding version of Conjecture 3.9 over $\mathbb{Z}/3$ does not hold. Also note that the slope of the rational component is no longer divisible by 4.

4. A table of invariants

In the following, we list the absolutely bigraded invariants $\varkappa$ for all strong inversions whose underlying knots have at most 9 crossings. We do this as follows: We subdivide the drawing plane into a grid and associate with each point on the plane a bigrading, namely the homological grading is equal to the x-coordinate and the

δ-grading is equal to the y-coordinate. Moving a point right and upwards increases both gradings. For each pair (K, h), we can write

$$\varkappa(K, h) = \bigoplus_i h^{a_i} \delta^{b_i} V_\varkappa$$

since all special components of the tangle invariants have length 2. Then, for each i, we place a grey box centred at the point (a_i, b_i). If multiple boxes line up at the same bigrading, we add a label which indicates the number of such boxes. Finally, the absolute bigrading is specified by the two numbers in the bottom left corner, which indicate the absolute coordinate of the bottom-and-left-most intersection point of the grid: The top-left number is the δ-grading, the bottom-right number is equal to the homological grading. For example,

$$\varkappa(4_1^1) = h^{2.5}\delta^{5.5} V_\varkappa \oplus h^{6.5}\delta^{4.5} V_\varkappa.$$

The superscripts $\spadesuit = 1, 2$ indicate the strong inversions, using the same numbering convention as in [8]. We follow the grading conventions in [5]; when comparing these computations to [10], note that our δ-grading has the opposite sign, and our quantum grading is twice as large.

Finally, we note that there is a mistake in the diagram for 9_{43} in Sakuma's tabulation [8], where the diagram given is an alternating knot of determinant 43 and Rasmussen's s-invariant ± 2. The only such knots with fewer than 10 crossings sharing these properties are 9_{21} and 9_{22}, according to knotinfo [7]; by comparing the $\varkappa$-invariant of the quotients, we see that Sakuma's diagram shows 9_{22}. A diagram for the knot 9_{43} is shown on the right. (Its determinant is 13 and $s = \pm 4$. The only other knot with fewer than 10 crossings with these properties is 7_3, but its strong inversions have different $\varkappa$ than the ones we compute for 9_{43}.) Changing the pair of shaded crossings indicated in the image on the right gives the diagram in Sakuma's table.

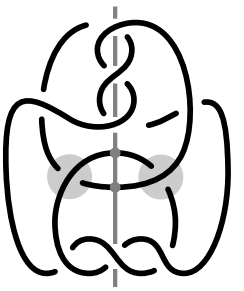

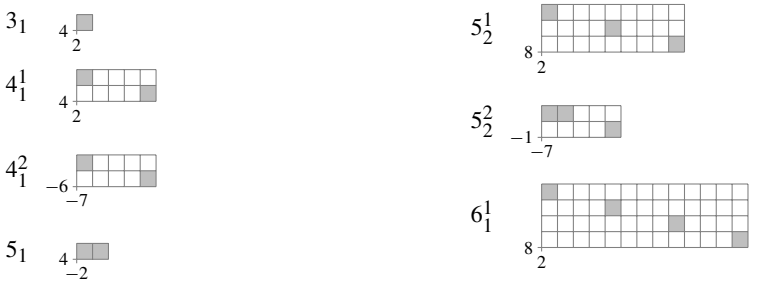

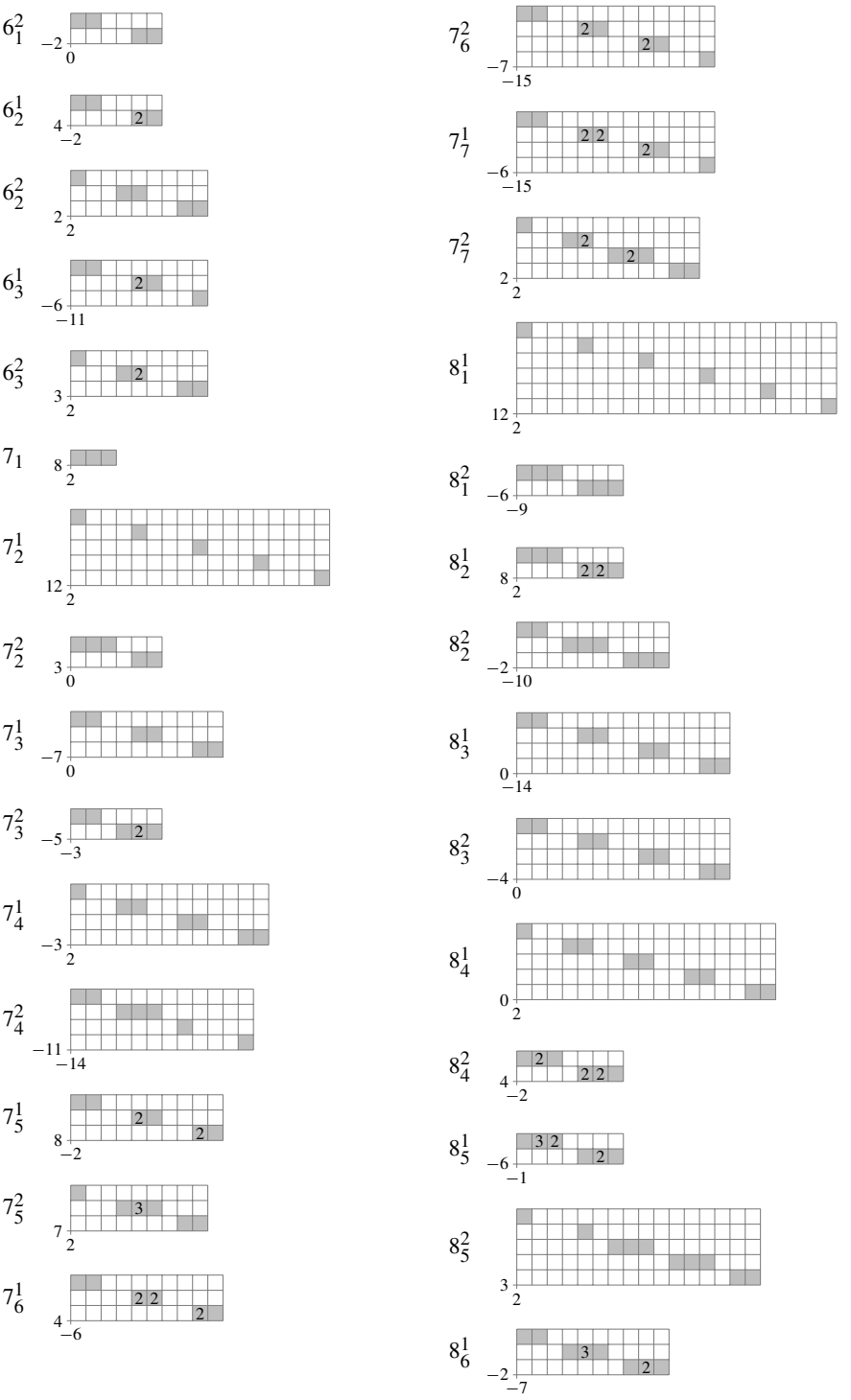
6_1^2
6_2^1
6_2^2
6_3^1
6_3^2
7_1
7_2^1
7_2^2
7_3^1
7_3^2
7_4^1
7_4^2
7_5^1
7_5^2
7_6^1
7_6^2
7_7^1
7_7^2
8_1^1
8_1^2
8_2^1
8_2^2
8_3^1
8_3^2
8_4^1
8_4^2
8_5^1
8_5^2
8_6^1

8^2_6 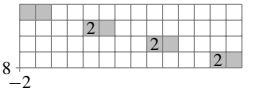

8^1_7 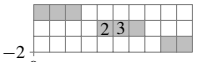

8^2_7 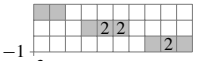

8^1_8 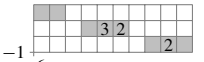

8^2_8 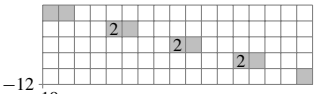

8^1_9 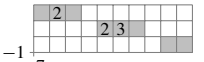

8^2_9 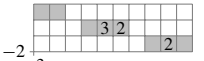

8_{10} 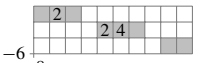

8^1_{11} 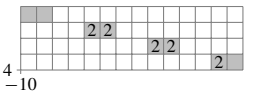

8^2_{11} 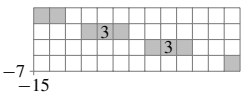

8^1_{12} 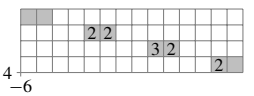

8^2_{12} 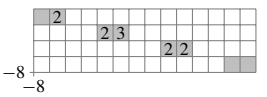

8^1_{13} 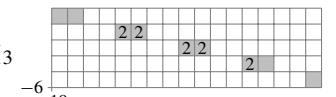

8^2_{13} 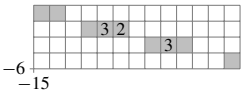

8^1_{14} 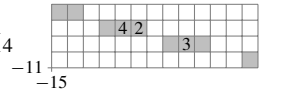

8^2_{14} 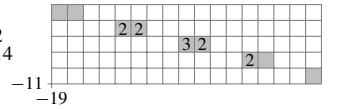

8^1_{15} 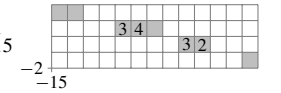

8^2_{15} 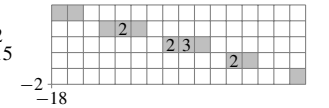

8_{16} 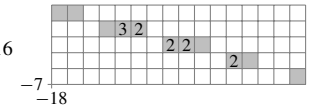

8^1_{18} 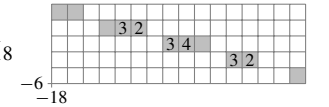

8^2_{18} 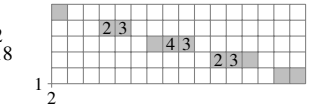

8_{19} 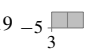

8_{20} 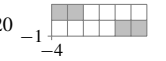

8^1_{21} 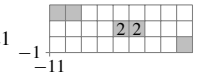

8^2_{21} 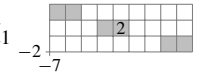

9_1 

9^1_2 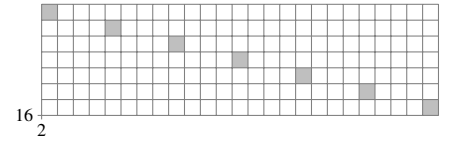

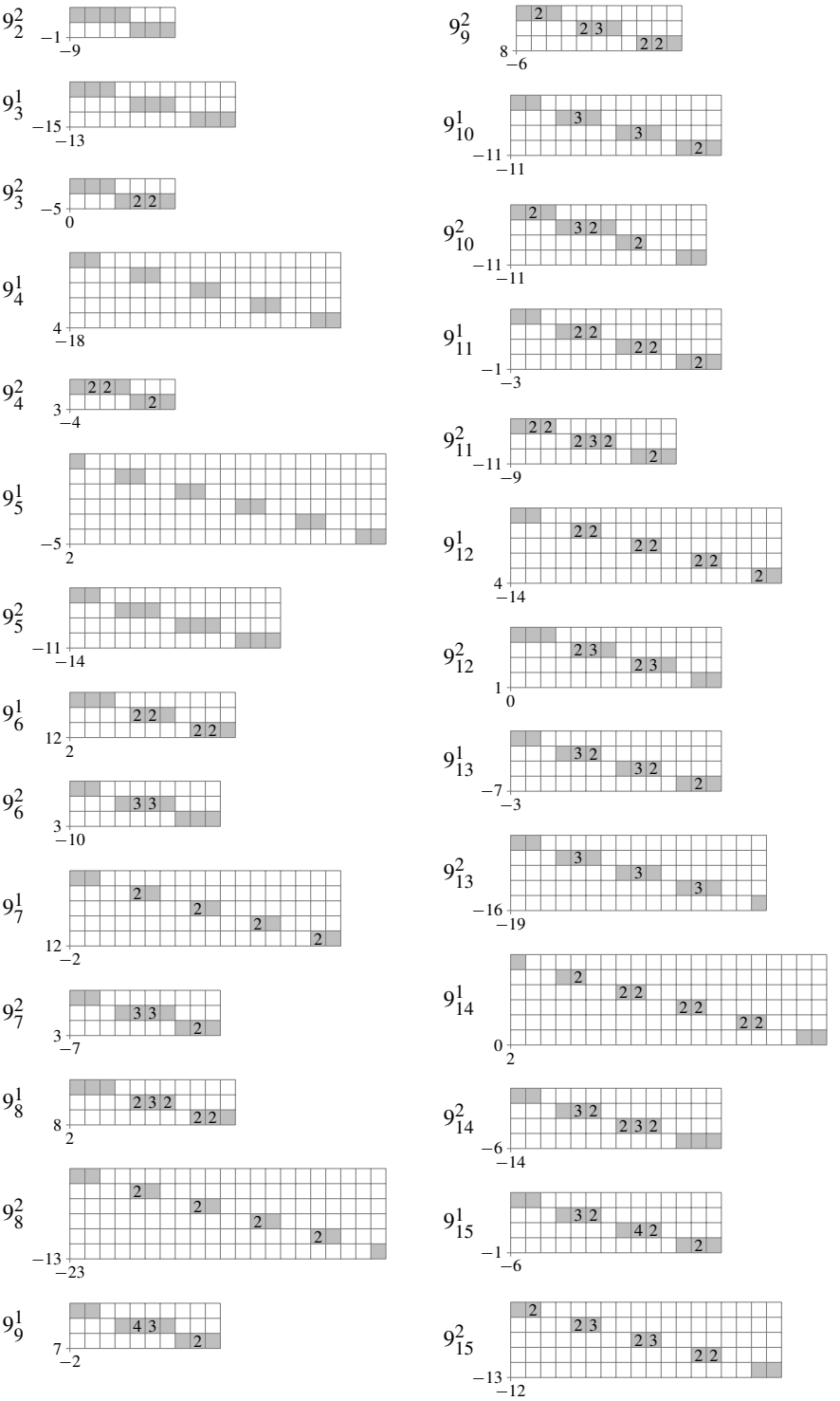
9^2_2 −1 −9
9^1_3 −15 −13
9^2_3 2 2 −5 0
9^1_4 4 −18
9^2_4 2 2 2 3 −4
9^1_5 −5 2
9^2_5 −11 −14
9^1_6 2 2 2 2 12 2
9^2_6 3 3 3 −10
9^1_7 2 2 2 2 12 −2
9^2_7 3 3 2 3 −7
9^1_8 2 3 2 2 2 8 2
9^2_8 2 2 2 2 −13 −23
9^1_9 4 3 2 7 −2
9^2_9 2 2 3 2 2 8 −6
9^1_{10} 3 3 2 −11 −11
9^2_{10} 2 3 2 2 −11 −11
9^1_{11} 2 2 2 2 2 −1 −3
9^2_{11} 2 2 2 3 2 2 −11 −9
9^1_{12} 2 2 2 2 2 2 4 −14
9^2_{12} 2 3 2 3 1 0
9^1_{13} 3 2 3 2 2 −7 −3
9^2_{13} 3 3 3 −16 −19
9^1_{14} 2 2 2 2 2 2 0 2
9^2_{14} 3 2 2 3 2 −6 −14
9^1_{15} 3 2 4 2 2 −1 −6
9^2_{15} 2 2 3 2 3 2 2 −13 −12

9^1_{16}
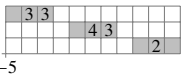

9^2_{16}
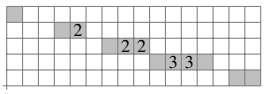

9^1_{17}
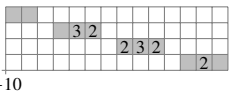

9^2_{17}
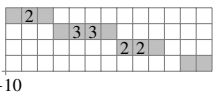

9^1_{18}
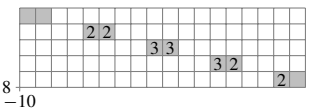

9^2_{18}
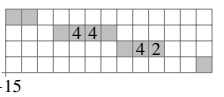

9^1_{19}
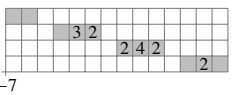

9^2_{19}
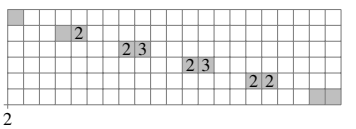

9^1_{20}
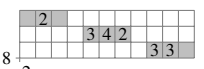

9^2_{20}
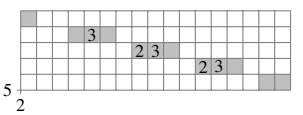

9^1_{21}
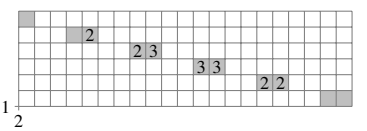

9^2_{21}
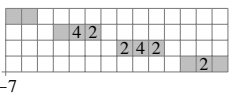

9_{22}
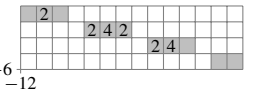

9^1_{23}
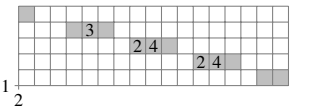

9^2_{23}
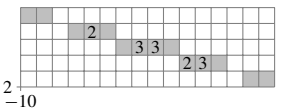

9_{24}
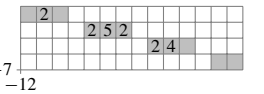

9_{25}
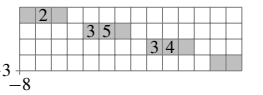

9^1_{26}
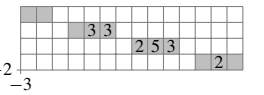

9^2_{26}
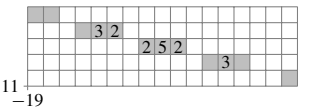

9^1_{27}
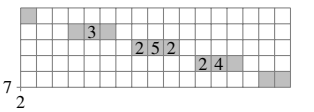

9^2_{27}
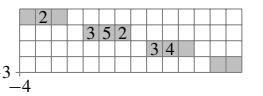

9^1_{28}
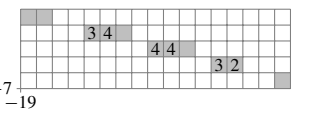

9^2_{28}
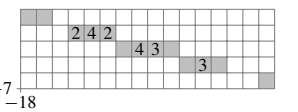

9_{29}
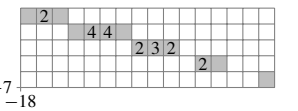

9_{30}

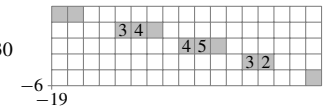

9^1_{31}

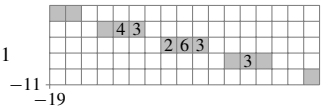

9^2_{31}

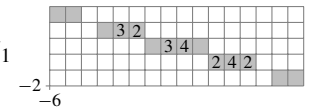

9_{34}

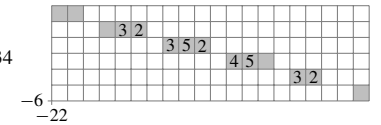

9^1_{35}

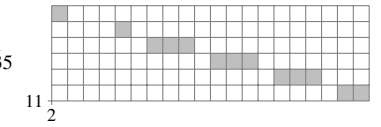

9^2_{35}

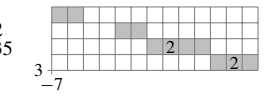

9_{36}

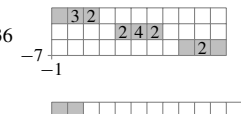

9^1_{37}

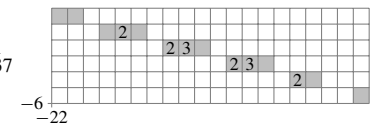

9^2_{37}

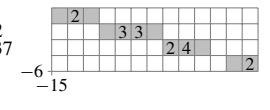

9_{38}

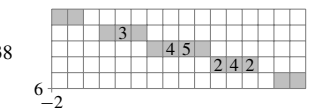

9_{39}

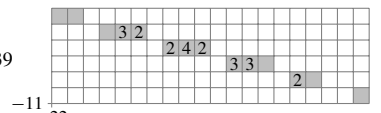

9^1_{40}

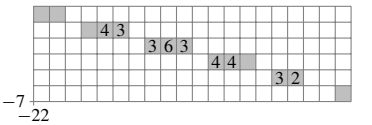

9^2_{40}

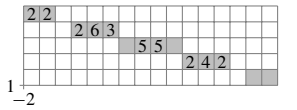

9_{41}

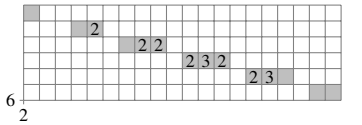

9_{42}

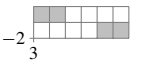

9_{43}

9_{44}

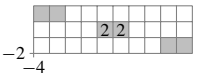

9_{45}

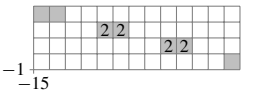

9^1_{46}

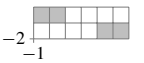

9^2_{46}

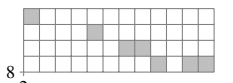

9_{47}

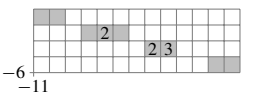

9^1_{48}

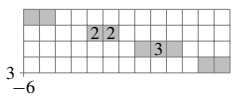

9^2_{48}

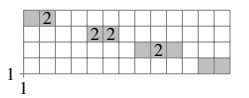

9_{49}

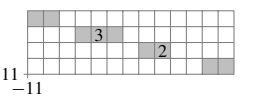

Acknowledgements

The computer program [12] used in this work represents a major overhaul to an earlier piece of software, developed as part of a UBC undergraduate research project with Gurkeerat Chhina.

References

[1] D. Bar-Natan, "Khovanov's homology for tangles and cobordisms", *Geom. Topol.* **9** (2005), 1443–1499. MR Zbl

[2] K. Boyle and A. Issa, "Equivariant 4-genera of strongly invertible and periodic knots", 2021. arXiv 2101.05413

[3] C. M. Gordon and J. Luecke, "Knots are determined by their complements", *J. Amer. Math. Soc.* **2**:2 (1989), 371–415. MR Zbl

[4] R. Hartley, "Knots and involutions", *Math. Z.* **171**:2 (1980), 175–185. MR Zbl

[5] A. Kotelskiy, L. Watson, and C. Zibrowius, "Immersed curves in Khovanov homology", 2019. arXiv 1910.14584

[6] A. Kotelskiy, L. Watson, and C. Zibrowius, "Khovanov multicurves are linear", 2022. arXiv 2202.01460v1

[7] C. Livingston and A. H. Moore, "KnotInfo: table of knot invariants", 2021, available at https://knotinfo.math.indiana.edu.

[8] M. Sakuma, "On strongly invertible knots", pp. 176–196 in *Algebraic and topological theories* (Kinosaki, 1984), Kinokuniya, Tokyo, 1986. MR Zbl

[9] L. Watson, "A remark on Khovanov homology and two-fold branched covers", *Pacific J. Math.* **245**:2 (2010), 373–380. MR Zbl

[10] L. Watson, "Khovanov homology and the symmetry group of a knot", *Adv. Math.* **313** (2017), 915–946. MR Zbl

[11] C. Zibrowius, "On symmetries of peculiar modules; or, δ-graded link Floer homology is mutation invariant", 2019. To appear in *J. Eur. Math. Soc.* arXiv 1909.04267

[12] C. Zibrowius, "`kht++`, a program for computing Khovanov invariants for links and tangles", April 2021, available at https://cbz20.raspberryip.com/code/khtpp/docs/.

Received 3 Mar 2021. Revised 18 Aug 2021.

ARTEM KOTELSKIY: `artofkot@gmail.com`
Mathematics Department, Stony Brook University, Stony Brook, NY, United States

LIAM WATSON: `liam@math.ubc.ca`
Department of Mathematics, University of British Columbia, Vancouver, BC, Canada

CLAUDIUS ZIBROWIUS: `claudius.zibrowius@posteo.net`
Faculty of Mathematics, University of Regensburg, Regensburg, Germany

Volume Editors:

John A. Baldwin
Boston College
Boston, MA
United States

Hans U. Boden
McMaster University
Hamilton, ON
Canada

John B. Etnyre
Georgia Institute of Technology
Atlanta, GA
United States

Liam Watson
University of British Columbia
Vancouver, BC
Canada

The cover image is based on an illustration from the article "Khovanov homology and strong inversions", by Artem Kotelskiy, Liam Watson and Claudius Zibrowius (see p. 232).

Electronic copies can be obtained free of charge from http://msp.org/obs/5 and printed copies can be ordered from MSP (contact@msp.org).

The Open Book Series is a trademark of Mathematical Sciences Publishers.

ISSN: 2329-9061 (print), 2329-907X (electronic)

ISBN: 978-1-935107-11-8 (print), 978-1-935107-10-1 (electronic)

First published 2022.

MATHEMATICAL SCIENCES PUBLISHERS
798 Evans Hall #3840, c/o University of California, Berkeley CA 94720-3840
contact@msp.org **https://msp.org**

THE OPEN BOOK SERIES 5

Gauge Theory and Low-Dimensional Topology: Progress and Interaction

This volume is a proceedings of the 2020 BIRS workshop *Interactions of gauge theory with contact and symplectic topology in dimensions 3 and 4*. This was the 6th iteration of a recurring workshop held in Banff. Regrettably, the workshop was not held onsite but was instead an online (Zoom) gathering as a result of the Covid-19 pandemic. However, one benefit of the online format was that the participant list could be expanded beyond the usual strict limit of 42 individuals. It seemed to be also fitting, given the altered circumstances and larger than usual list of participants, to take the opportunity to put together a conference proceedings.

The result is this volume, which features papers showcasing research from participants at the 6th (or earlier) *Interactions* workshops. As the title suggests, the emphasis is on research in gauge theory, contact and symplectic topology, and in low-dimensional topology. The volume contains 16 refereed papers, and it is representative of the many excellent talks and fascinating results presented at the Interactions workshops over the years since its inception in 2007.

TABLE OF CONTENTS